Sensors & Transducers, Vol. 178, Issue 9, September 2014, pp. 219-225

Sensors & Transducers

Study on Magneto-Hydro-Dynamics Disturbance Signal Feature Classification Using Improved S-Transform Algorithm and Radial Basis Function Neural Network

[1, 2] Nan YU, [1] Jiarong LUO
[1] School of Information Science & Technology, Donghua University, Shanghai, 201620, China
[2] College of Information and Technology, Shanghai Maritime University, Shanghai, 201306, China
[1] E-mail: yun@shmtu.edu.cn

Received: 21 June 2014 /Accepted: 29 August 2014 /Published: 30 September 2014

Abstract: The interference signal in magneto-hydro-dynamics (MHD) may be the disturbance from the power supply, the equipment itself, or the electromagnetic radiation. Interference signal mixed in normal signal, brings difficulties for signal analysis and processing. Recently proposed S-Transform algorithm combines advantages of short time Fourier transform and wavelet transform. It uses Fourier kernel and wavelet like Gauss window whose width is inversely proportional to the frequency. Therefore, S-Transform algorithm not only preserves the phase information of the signals but also has variable resolution like wavelet transform. This paper proposes a new method to establish a MHD signal classifier using S-transform algorithm and radial basis function neural network (RBFNN). Because RBFNN centers ascertained by k-means clustering algorithm probably are the local optimum, this paper analyzes the characteristics of k-means clustering algorithm and proposes an improved k-means clustering algorithm called GCW (Group-cluster-weight) k-means clustering algorithm to improve the centers distribution. The experiment results show that the improvement greatly enhances the RBFNN performance. *Copyright © 2014 IFSA Publishing, S. L.*

Keywords: S-Transform algorithm, Magneto-hydro-dynamics (MHD), Radial basis function neural network, Short time Fourier transform, Wavelet transform.

1. Introduction

In HT-7 Tokamak discharge tests, the magnetohydrodynamics (MHD) signals acquisition is by using Maher probes. The magnetic field plasma flow makes the saturation ion current at the direction of paralleling to the Maher probe surface unequal to that at the inverse direction. Maher probes use this unequal to measurement the plasma flow velocity. The definition of the plasma Maher number paralleling to the magnetic field direction is:

$$H = v_z / v_s = v_z / [k(C_i + C_e)/m_i]^{1/2}, \quad (1)$$

C_i is the ion temperature, C_ε is the electron temperature, m_i is the ion mass, K is the Boltzmann constant, v_z is the ion drift velocity, and v_s is the ion velocity.

Fig. 1 expresses the Maher probes used in the Tokamak HT-7. Probe No. 1 and No. 7 distributed function is metering upstream and downstream saturation ion current value. The physical distance between probe No. 5 and probe No. 6 is 5 mm. According to delay time, the plasma poloidal rotation velocity can be calculated through their measurement.

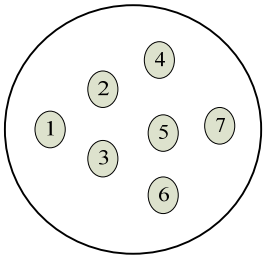

Fig. 1. Schematic diagram of the Maher probe model.

Because the discharge and acquisition equipment working environment is not a vacuum environment, the collected signals often contain interference signals. These disturbance signals sometimes can cause mutation of the output signals. It has great difficulties to distinguish the mutation signals which are caused by the magnetic fluid instability from those caused by interference. Fig. 2 is one of signals acquisition results. The No. 1 signal mutation is caused by the magnetic fluid instability, another No. 2 is the mutation signal caused by composition of magnetic fluid instability and interference, and the third mutation is caused by signal interference.

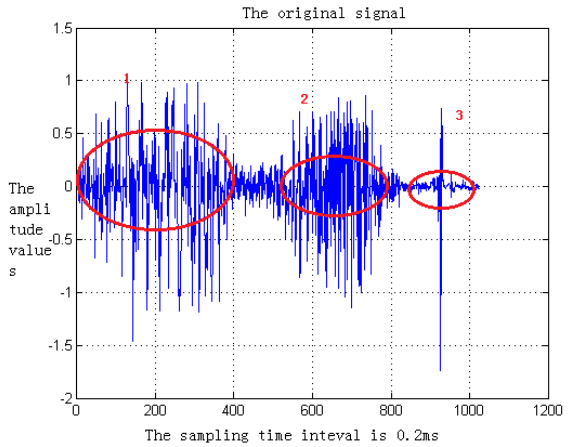

Fig. 2. Discharge sampling magnetic fluid unstable signal.

To distinguish the interference signal is very important for plasma discharge. In recent research, wavelet transform (WT) is widely applied in analyzing unstable signals for enhancing signals quality assessment [2-4]. Although the identification efficiency is significantly improved, the effect of disturbance signals does not give full consideration in many cases. [5] shows that MLP neural network on the basis of wavelet transform has poor performance because of the disturbance of noise. [6] proposes a noise-reduction method to increase the efficiency of signal pattern recognition. In paper [7], it presents two frequency-domain implementations of the shift-invariant periodic discrete wavelet transform (SI-DWT) and it's inverse. The paper experimentally demonstrates the reduction in computation time achieved by the direct frequency domain implementation of the SI-DWT for wavelet filters with non-compact support.

The method of this article is to apply an improved S-transform algorithm to distinguish interference pulse spikes from instability ones. The S-transform algorithm (ST) proposed by Stockwell [8] in 1996, which is the development of Gabor and wavelet transform. ST adopts variable width Gauss window, whose time window width is inversely proportional to the variation of the frequency. The time window is wider in low frequency, and narrow in high frequency, so we can achieve very high time resolution. Thus the transform can observe some small part of the signal, which overcomes some defects of FFT and wavelet transform. At the same time, ST has close contact with the Fourier transform, whose time frequency has relations with frequency. We can use Fourier transform and convolution theorem to accomplish ST with the help of existing Fast Fourier transform (FFT).

The ST algorithm is applied in many fields, including signal processing, fault diagnosis, vibration power, earthquake prediction, medicine and other fields, and many papers have been published [9-11]. The paper[12] proposes a novel high-performance classification system based on the S-transform and a probabilistic neural network (PNN). The original power quality signals are analyzed by the S-transform and processed into a complex matrix named the S-matrix. Eighteen types of time–frequency features are extracted from the S-matrix. The simulation results show that 8 types of PQ disturbance signals with 2 types of complex disturbances are classified precisely and that the new PNN-based approach more accurately classified PQ disturbances compared to back propagation neural network (BPNN) and radial basis function neural network (RBFNN) approaches. Power quality is one of the major issues in the modern electrical power world. The widespread usage of power electronic devices and non-linear loads make the power system more vulnerable to the power quality disturbances. As the power grids are expanding more and more because of the renewable sources, it necessitates responsive detection and accurate classification of power quality disturbances for corrective measures. Paper[13] presents a new approach for power quality analysis using an orthogonal time–frequency representation of S-transform called Discrete Orthogonal S-transform (DOST). Different power quality disturbances have been analyzed using the short time Fourier transform (STFT), discrete wavelet transform (DWT), S-transform (ST) and DOST. Different case studies validate the superiority of DOST over other transforms in a more efficient way to monitor the power quality disturbances.

2. The Improved S-transform Algorithm

The S-Transform of signal $h(t)$ is defined as an equation (2).

$$S(\tau, f) = \int_{-\infty}^{\infty} h(t) \frac{|f|}{\sqrt{2\pi}} e^{-(\tau-t)^2 f^2/2} e^{-i2\pi ft} dt \quad (2)$$

,

If S-Transform indeed represents the local spectrum, we can simply obtain the Fourier spectrum on the local spectrum average in the time axis. In equation (3), $H(f)$ is the Fourier transform of $h(t)$.

$$\int_{-\infty}^{\infty} S(\tau, f) d\tau = H(f) \quad (3)$$

,

$h(t)$ can be recovered by $S(\tau, f)$.

$$h(t) = \int_{-\infty}^{\infty} \left\{ \int_{-\infty}^{\infty} S(\tau, f) d\tau \right\} e^{i2\pi ft} df \quad (4)$$

,

From here we can see that the obvious difference between S-Transform and wavelet transform. S-Transform is an instant frequency (IF) extended to the wideband signal. The one dimensional function and the fixed parameter f_1 of variable τ defined by the $S(\tau, f_1)$ is called a sound. The sound with specified frequency f_1 can be defined as:

$$S(\tau, f_1) = A(\tau, f_1) e^{i\Phi(\tau, f_1)} \quad (5)$$

,

Because a sound expresses a divided special section, we can define the instantaneous frequency of IF using phase:

$$IF(\tau, f_1) = \frac{1}{2\pi} \frac{\partial}{\partial t} \{2\pi f_1 \tau + \Phi(\tau, f_1)\} \quad (6)$$

,

S-Transform can be rewritten using $h(t)$ Fourier spectrum signal $H(t)$ as:

$$S(\tau, f) = \int_{-\infty}^{\infty} H(\alpha + f) e^{-2\pi^2 \alpha^2 / f^2} e^{j2\pi\alpha\tau} d\alpha \quad f \neq 0 \quad (7)$$

,

The discrete simulation of equation (7) uses the convenience and convolution theory of fast Fourier transform (FFT) to compute the discrete S-Transform. Do not need to transform into a cosine curve, S-Transform can calculate the real and imaginary part of the amplitude spectrum and phase spectrum.

$h[kT], k = 0,1,\cdots, N-1$ represents the signal discrete sampling points, and the sampling interval is T. The discrete Fourier transform can be written as:

$$H\left[\frac{n}{NT}\right] = \frac{1}{N} \sum_{k=0}^{N-1} h[kT] e^{-i2\pi nk/N} \quad n = 0,1,\cdots, N-1 \quad (8)$$

Discrete S-Transform is a vector which is defined by dispersing $h[kT]$ into a series of derived vector along the time axis. These derivative vectors are not orthogonal to each other, and are not independent. Each basis vector is partitioned into N local vectors. The segmentation method is through N adjustable Gauss window. The sum of N segmented local vector is the original basis vector. Discrete signal $h[kT]$ S-Transform can be defined as ($f \to n/NT$ *and* $\tau \to jT$):

$$s[jT, \frac{n}{NT}] = \sum_{m=0}^{N-1} H[\frac{m+n}{NT}] e^{\frac{-2\pi^2 m^2}{n^2}} e^{\frac{i2\pi mj}{N}} \quad n \neq 0 \quad (9)$$

When $n = 0$ the equation (9) is equivalent to:

$$s[jT, 0] = \frac{1}{N} \sum_{m=0}^{N-1} h(\frac{m}{NT}) \quad j, m, and \quad n = 0,1,\cdots, N-1 \quad (10)$$

The above formula brings the average time series values into a zero frequency sound, so that the inverse transform is accurate. Discrete S-Transform has the same sampling and finite length problem, thus it lengthens the implicit cycle of the time and frequency domain. The discrete S-Transform transform inversion is:

$$h[kT] = \sum_{n=0}^{N-1} \left\{ \frac{1}{N} \sum_{j=0}^{N-1} S\left[jT, \frac{n}{NT} \right] \right\} e^{i2\pi nk/N} \quad (11)$$

,

Fourier transform spectrum using the Gauss window with a particular parameter n is called Gauss sound. Any S-Transform sound can be calculated by the time axis of the Fourier spectrum and Gauss sound. The Gauss sound is defined as:

$$G(m, n) = e^{-\frac{m^2}{2\left(\frac{n}{2\pi}\right)^2}} \quad (12)$$

,

Because the sampling is carried out on a time axis, so the discrete spectrum has timeliness.

This paper has introduced the basic principle of S-Transform, and showed the advantages of S-Transform algorithm in the analysis of signals. But the S-Transform algorithm resolution in the high frequency is still not clear. Standard deviation of Gauss window depends on the frequency, so the standard deviation is adjusted to improve the energy concentration.

Standard deviation is the function of frequency, it is defined in the Stockwell S-Transform algorithm article in 1996:

$$\sigma(f) = \frac{1}{|f|}, \quad (13)$$

Equation (2) can be rewritten as:

$$S(\tau, f) = \int_{-\infty}^{\infty} h(t) \frac{1}{\sigma(f)\sqrt{2\pi}} e^{\frac{-(t-\tau)^2}{2\sigma^2(f)}} e^{-i2\pi ft} dt, \quad (14)$$

The S-Transform result is showed in Fig. 3. The result shows the high frequency resolution is not high enough.

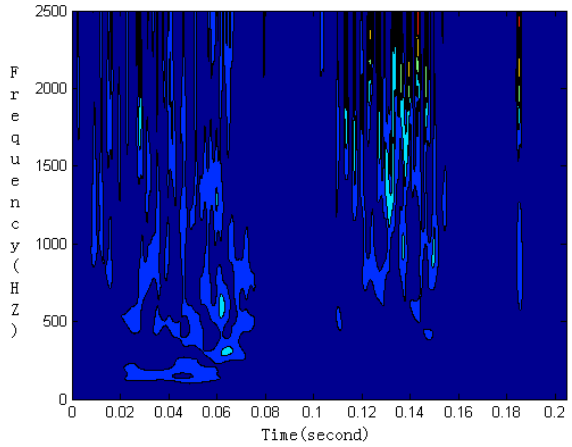

Fig. 3. S-Transform ending.

In the Sejdic, Djurovic, and Jiang 2008's article, window standard variance was adjusted as below:

$$\sigma(f) = \frac{1}{|f|^p} \qquad 0 \le p \le 1, \quad (15)$$

The adjusted S-Transform is:

$$S(\tau, f) = \int_{-\infty}^{\infty} h(t) \frac{|f|^p}{\sqrt{2\pi}} e^{\frac{-(t-\tau)^2 |f|^p}{2}} e^{-i2\pi ft} dt, \quad (16)$$

The parameter p acts like a switch. When p=0, the equation (16) is the short time Fourier transform, if p=1, it is the S-Transform. But experiments show an interesting phenomenon that the change of parameter p between the 0 and 1 makes transformation obtaining the better time-frequency resolution. p<0 cannot be used, because it would cause the standard variance proportional to frequency which is out of line with S-Transform definition.

The improvement by adjusting the window size enhances the high frequency resolution. Experiments show that p=0.8 gains the best high frequency resolution (Fig. 4). From the resolution image, this paper can draw a comprehensive conclusion that the improved S-Transform algorithm obtains optimal signal resolution.

Frequency features are extracted from the S-transform matrix. Then these features are provided to radial basis function neural network for classification as input vectors.

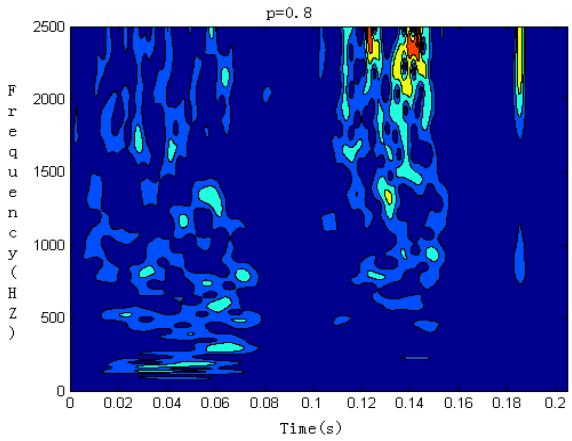

Fig. 4. p=0.8, S-Transform ending.

3. Radial Basis Function Neural Network (RBFNN) Algorithm

3.1. RBFNN Architecture

RBFNN is a novel and efficient adaptive feed forward neural network, it has the best fitting ability, the faster training speed, no problem of immersing into the partial least point. All these merits make RBFNN be widely used in non-linear time series prediction. Powell proposed multivariate interpolation Radial-Basis Function (RBF) algorithm in 1985. Broomhead and Lowe applied RBF to designing neural networks. RBFNN mappings low-dimensional input vectors in high-dimension data space, and uses weighted summation of the outputs of hide cells to get the final result.

Feed forward RBFNN had three layers. The first one is input-layer composed of signal source nodes. The second one is the hide-layer. In this layer, nodes transform function is a local distribution of nonnegative nonlinear function which is the center-point radial symmetry and attenuation. The numbers of hide-layer nodes are determined by the questions. The third layer is the output-layer. The consequences of the output-layer are hiding-layer results linear weight numbers. The transformation from the input space to hide-layer space is nonlinear but it is linear from hiding-layer space to output-layer space. The RBFNN architecture is expressed in Fig. 4. $X = [x_i \mid i = 1,2,\ldots N]^T$ is a input vector, $\{\varphi_i(x) \mid i = 1,2,\ldots m\}$ is a group of radial basis functions, $\{w_i \mid i = 1,2,\ldots m\}$ is a set of weightings, b is offset.

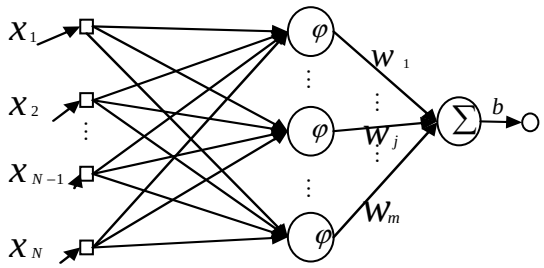

Fig. 5. RBFNN Architecture.

3.2. RBFNN Algorithm

The RBFNN accepts training samples $X = \left[\chi_i \mid i = 1,2,\ldots N\right]^T$ and approximation function is an equation (17)

$$F(x) = \sum_{i=1}^{m} w_i \varphi_i(x) \quad , \tag{17}$$

$\{w_i \mid i = 1,2,\ldots m\}$ is a set of weightings, and they are linearly independent each other. $\varphi_i(x) = G(\| x - t_i \|)$, $i = 1,2,\cdots m$ is a center set which is needed to be confirmed. $G(\cdot)$ usually uses Gauss function because of simple representation, radial symmetry, good smoothness with any number derivatives. The cost function is expressed as an equation (18):

$$\xi(F) = \sum_{i=1}^{N} (d_i - \sum_{j=1}^{m} w_j G(\| x_i - t_j \|))^2 + \lambda \| DF \|^2 \quad , \tag{18}$$

$$\| DF \|^2 = \sum_{j=1}^{m} \sum_{i=1}^{m} w_j w_i G(t_j, t_i) \quad , \tag{19}$$

When regularization parameter λ approaches zero, weight vector w is expressed as

$$w = (G^T G)^{-1} G^T d \quad , \tag{20}$$

$$d = [d_1, d_{2,\cdots,} d_N]^T \quad , \tag{21}$$

$$w = [w_1, w_{2,\cdots,} w_m]^T \quad , \tag{22}$$

$$G = \begin{bmatrix} G(x_1,t_1) & G(x_1,t_2) & \cdots & G(x_1,t_m) \\ G(x_2,t_1) & G(x_2,t_2) & \cdots & G(x_2,t_m) \\ \vdots & \vdots & \vdots & \vdots \\ G(x_N,t_1) & G(x_N,t_2) & \cdots & G(x_N,t_m) \end{bmatrix}, \tag{23}$$

4.2. Methods of Ascertaining RBFNN Centers

In the learning process of radial basis function network, it should adopt different learning strategies on the activation function centers and linear weight because the hidden layer activation function center updating is very slow and the linear weight connected to the output layer is quick because of the optimal learning and updating strategies. According to the activation function center updating methods, it can use different learning strategies to construct radial basis function neural networks. The main construction ways include that constant center specification randomly, self organizing center selection method and supervisory center selection method.

4.3. Applying K-means Algorithm to Ascertain RBFNN Centers

K-Means algorithm is a kind of non-supervision indirect clustering method which is based on sampling data similarity-rate. It divides data n into k clustering which has high similarity in the same class and low similarity in different classes. The K-means algorithm is

Input: the cluster number k, data matrix N

Output: clustering k which has the least square error

1) Selecting k vectors randomly as original clustering centers. c_1^1, c_2^1, …, c_k^1

2) Computing distances from every vector to clustering centers.

$$d_{ij} = \left(v_i - c_j^p\right)^2 (i = 1\cdots n, j = 1\cdots k, p = 1)$$

Selecting the smallest distance $\min$ and classifying the v_i into cluster c_{pj}

3) Calculating the average of all objects as new clustering centers for every class.

4) Redistributing all data and objects according to the distance to clustering centers.

5) p=p+1, return to 3 until the objective function is no longer changed.

4.4. Applying Improved Algorithm GCW-k-Means Algorithm to Ascertain RBFNN Centers

GCW-k-means algorithm is an improved k-means algorithm which grouped and clustered the training data and adjusted the centers by weight which provided by experts. The GCW-k-means is:

Input: the cluster number k, group number g, data matrix N,

Output: clustering k which has the least square error.

1) Dividing training data to group g by sampling.

2) For every group q (q=1 to g), selecting k vectors randomly as original clustering centers,

$$C_{q1}^{1},\quad C_{q2}^{1},\quad \cdots,\quad C_{qk}^{1}(q=1\ \ to\ \ g)$$

3) Applying k-means algorithm on every group and then obtaining every group clustering centers

$$C_{q1}^{p},\quad C_{q2}^{p},\quad \cdots,\quad C_{qk}^{p}(q=1\ \ to\ \ g)$$

4) For every group centers, experts provided an evaluation weight vector $ew_q=[w_{q1},w_{q2}\ldots w_{qk}](q=1\ \ to\ \ g)$ according to the group centers.

5) The final k clustering centers are ascertained by

$$C=[C_i]=\frac{\sum_{q=1tog} ew_q\cdot c_q}{\sum_{q=1tog} ew_q}(c=1\ \ to\ \ k)$$

The experiments showed in Figs. 6-7.

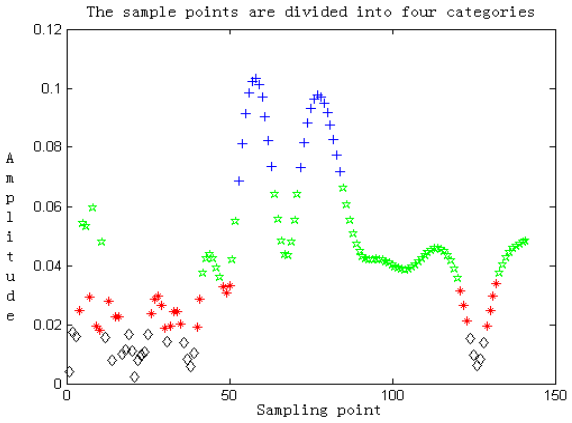

Fig. 6. The sample points are divided into 4 class using GCW-k-means algorithm.

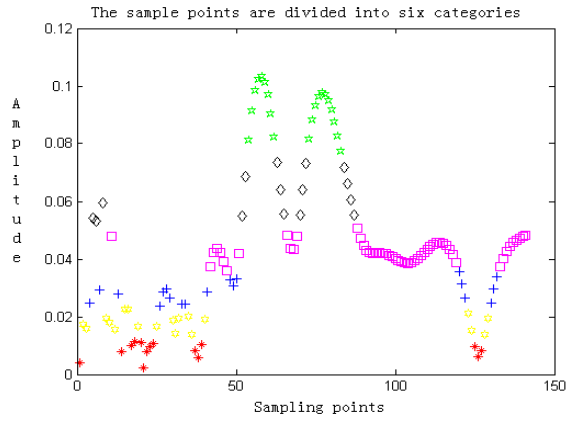

Fig. 7. The sample points are divided into 6 class using GCW-k-means algorithm.

5. Discussion

This paper has proposed an approach for diagnosing, classifying and characterizing of non-stationary nuclear fusion discharging device signals using the improved S-transform and modified RBFNN classifier. The S-transform was used to generate frequency-amplitude distributions and key features are derived for classification. But depending on S-transform solely could not distinguish disturbance signals from normal ones completely. Radial Basis Function Neural Network is applied to recognize the disturbance. The determination of centers is adopted GCW-k-means algorithm which derived from k-means algorithm. Experiment shows RBFNN with GCW-k-means algorithm has a better recognition deviation

Acknowledgments

This work is supported by National Science Foundation of China (No. 10875027) and the National Natural Science Foundation of China under Grant No. 61202022.

References

[1]. Zhao Da-Zheng, Luo Jia-Rong, Li Gang, Update of Plasma Density Feedback Control System in HT-7 Tokamak, *Nuclear Science and Techniques*, 2004, Vol. 15, Issue 4, pp. 232-235.

[2]. Carmen Capilla, Application of the Haar wavelet transform to detect microseismic signal arrivals, *Journal of Applied Geophysics*, 2006, Vol. 59, pp. 36–46.

[3]. Yanxue Wang, Zhengjia He, Yanyang Zi, Enhancement of signal denoising and multiple fault signatures detecting in rotating machinery using dual-tree complex wavelet transform, *Mechanical Systems and Signal Processing*, 2010, Vol. 24, pp. 119–137.

[4]. A. Meije Wink, J. B. T. M. Roerdink, Polyphase decompositions and shift-invariant discrete wavelet transforms in the frequency domain, *Signal Processing*, 2010, Vol. 90, pp. 1779-1787.

[5]. P. K. Dash, Nayak Maya, M. R. Senapati, I. W. C. Lee, Mining for similarities in time series data using wavelet based feature vectors and neural networks, *Eng. Appl. Artif. Intell*, 2007, Vol. 20, pp. 185-201.

[6]. H. T. Yang, C. C. Liao, A de-noising scheme for enhancing wavelet-based power quality monitoring systems, *Power Delivery*, 2001, Vol. 16, pp. 353-360.

[7]. H. Zang, P. Liu, O. P. Malik, Detection and classification of power quality disturbances in noisy conditions, *IEEE Proc.: Gener. Transm. Distrib.*, 2003, Vol. 150, Issue 5, pp. 567-572.

[8]. R. G. Stockwell, A basis for efficient representation of the S-transform, *Digital Signal Processing*, 2006, pp. 1-22.

[9]. C. R. Pinnegar, L. Mansinha, The S-transform with windows of arbitrary and varying shape, *Geophysics*, 2003, Vol. 68, Issue 1, pp. 381-385.

[10]. Ervin, Djurovi, Jin Jiang, A window width optimized S-transform, *EURASIP Journal on Advances in Signal Processing*, 2008, pp. 1-13.

[11]. Pinnegar C. R., Mansinha L., The bi-Gaussian S-transform, *SIAM Journal of Scientific Computing*, Vol. 24, No. 5, 2003, pp. 1678-1692.
[12]. Nantian Huang, Dianguo Xu, Xiaosheng Liu, Lin Lin, Power quality disturbances classification based on S-transform and probabilistic neural network, *Neurocomputing*, 2012, Vol. 98, pp. 12-23.
[13]. M. Jaya Bharata Reddy, R. Krishnan Raghupathy, K. P. Venkatesh, D. K. Mohanta, Power quality analysis using Discrete Orthogonal S-transform (DOST), *Digital Signal Processing*, 2013, Vol. 23, pp. 616-626.
[14]. F. Fernandez Navarro, C. Hervás Martínez, J. Sanchez Monedero, P. A. Gutierrez, MELM-GRBF: A modified version of the extreme learning machine for generalized radial basis function neural networks, *Neurocomputing*, 2011, Vol. 74, pp. 2502–2510.
[15]. Yuehui Chen, Jingru Xu, Bin Yang, Yaou Zhao, Wenxing He, A novel method for prediction of protein interaction sites based on integrated RBF neural networks, *Computers in Biology and Medicine*, 2012, Vol. 42, pp. 402–407.
[16]. Qu Yi, Li Zhan-Ming, Li Er-Chao, Fault detection and diagnosis for non-Gaussian stochastic distribution systems with time delays via RBF neural networks, *ISA Transactions*, 2012, Vol. 51, pp. 786–791.